ASSESSMENT OF SCELIC BASED HIGH-POWER BIDIRECTIONAL DC-DC CONVERTER FOR EFFECTIVE ENERGY MANAGEMENT IN PHEV

L.S. GNANA VANITHA
Research Scholar, Anna University, Chennai, Tamil Nadu, India
gnanavanithaapeeee@gmail.com

Dr. R. JEYABHARATH
Professor and Head of EEE Department, KSR Institute for Engineering and Technology, Tamil Nadu, India

Abstract: *In this paper novel self-computational emotional learning based intelligent controller is proposed for battery charging control in Plug in Hybrid Electric Vehicle (PHEV). PHEV plays a significant role in world's vehicle market for its reduced fuel consumption and less emission of gasoline. The large capacity of a battery in PHEV reduces fuel consumption, but it is an unexpected load in a residential power system. It may cause a Voltage drop in a power system in case of uncoordinated charging of many PHEVs at a time. A high power bidirectional DC-DC converter is introduced in PHEV to charge the battery when the motor in PHEV acts as a generator. Effective of charging of battery reduces the load to the grid which is proposed by novel SCELIC controller in this paper. Effectiveness of the proposed system is simulated using Matlab and compared to the Adaptive neuro-fuzzy controller based charging system. This paper proposes a method to reduce load demand on the distribution grid.*

Key words: *Plug in Hybrid Electric Vehicles (PHEV), ANFIS, SCELIC, Bidirectional converter, Battery Energy Storage System.*

1. Introduction.

The transportation sector is a major consumer of fossil fuel and emanates a high amount of pollution [1]. A recommended solution for this crisis necessitates motivating the higher use of electrified vehicles. Electrified vehicles are categorized as Electric vehicle, Hybrid electric vehicle and Plug in Hybrid electric vehicle. PHEVs have the additional ability to store energy from the electricity grid, using large capacity batteries. The energy stored can drive the vehicle on short trips, by this means it reduces vehicle's dependency on petroleum and potentially CO2 emissions. The major aspect with the PHEV is an abridged discharge of CO2 [2]. The discharge rate of CO2 by different types of vehicles per annum is shown in figure 1. The utilization of PHEV lessen increasing Green House Gas discharges from 2010 to 2050 can vary from 3.4 to 10.3 billion metric tons. The main feature with the PHEV is a reduced discharge of CO2 [2].

PHEVs offer the potential to lessen both gasoline utilization and related emissions. Compared to a HEV battery of PHEV is larger and more powerful motor is used in PHEV [3]. PHEVs are charged by either plugging into electric outlets [4] or by means of on-board electricity generation. Charging of PHEV increases the load on the distribution grid [5].

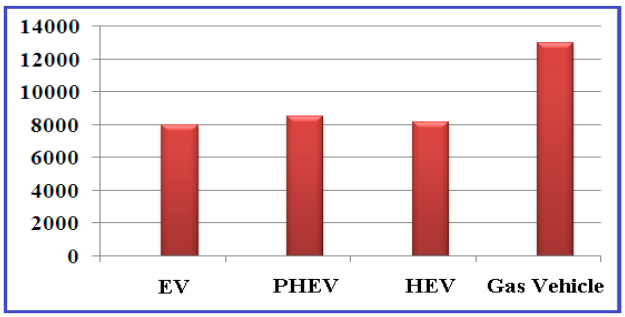


Fig. 1. Emission of CO_2 by vehicles per annum.

Unplanned charging of PHEVs in grid causes a voltage drop which reduces the quality of power in a grid. Since battery of PHEV is larger power consumption is high so in order to maintain power quality and reduces energy consumed from the grid efficient charging of a battery is discussed in this paper. The power use can be downplayed when the battery is turned on using some other sources instead of from the grid. In the period of regenerative braking or when the motor runs above the rated speed the motor works as a generator. This ability can be used to charge the battery in PHEV. For this dual active bridge is proposed in this paper. The dual active bridge is a bidirectional, controllable, dc-dc converter that has high power abilities consists of a high frequency transformer, eight switching devices, dc-link capacitors, and energy transfer inductor. By reason of the symmetry of this converter, with indistinguishable primary and secondary bridges, it is competent of bidirectional power flow control and the cause why it is chosen for PHEV. Modeling of dual active bridge bidirectional converter is analyzed by F. Krismer in 2010 [6]. Chenhao Nan; Ayyanar, R Analyzed PWM control technique for DAB in solid state transformer applications [7].

Various Design schemes and Techniques to Improve the Performance of a Dual Active Bridge with Phase-Shift Control is analyzed by Rodriguez, A et al., in 2015 [8]. High-Efficiency Dual-Active-Bridge DC/DC Converters is discussed with its switching losses by

BUPT

Ortiz, G.et.al by 2013 [9]. This paper uses this DAB converter to supply power from battery to motor and motor to the battery.

Battery energy storage system supports the performance of PHEV. Charging time of the battery is a significant factor in energy storage system. Charging controller plays a crucial role in BESS. ANFIS is an intelligent controller applied to various control applications.

ANFIS is applied as charging controller to improve charging performance. An emotional learning algorithm is an artificial intelligence control technique mimics human brain introduced by Lucas in 2004 [10]. An emotional controller is analyzed for various applications such as drives, heat exchangers, etc. In this paper novel Self-Computational Emotional Learning based Intelligent Controller (SCELIC) is proposed as charging controller. Performance SCELIC is compared with the ANFIS based charging controller.

2. DAB in PHEV

The bi-directional converter is introduced between the battery and motor. DAB consists of two converters both can act as a rectifier and an inverter. In case of battery act as a source the converter 1 act as an inverter and converter2 act as a rectifier. In case of battery charging, the converter 1 act as a rectifier and converter2 act as an inverter.

2.1 Basic Principle of Operation of DAB Converter

The DAB converter shown in figure 2 consists of an isolation transformer connects two full-bridge converters and a coupling inductor L, which may be provided partly or entirely by the transformer leakage inductance.

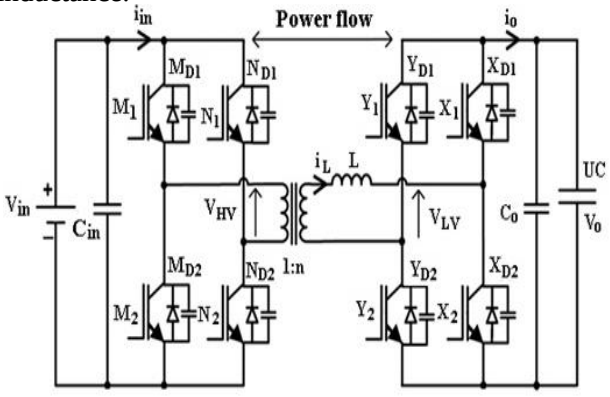


Fig. 2. Schematic of the DAB DC-DC converter.

The topology is shown in Fig. 2, where Vin and $Vout$ are the dc-link voltages, L is the coupling inductor, M1-2, N1-2, X1-2, Y1-2, are the controllable semiconductor switches. The low-voltage (LV) motor is connected to the full bridge on the right hand side and the HV DCs bus is connected to a full bridge on the left hand side of figure 2.

Each converter consists of two arms with two switching devices per arm, which are controlled with opposite square-wave pulses. In the dual active bridge, Power flow can be controlled by phase-shifting the pulses of one bridge as regards the other. This method of control, called phase shift modulation (PSM), controls power flow amid the two dc busses such that the lagging bridge receives power from the leading bridge [11]. Thus, bidirectional power flow is allowed via a small, lightweight High Frequency transformer and inductor combination, and power flows from the bridge generating the leading square-wave.

For high power operation even though diverse modes of operation of the DAB converter have been discussed recently [12-14], the square-wave mode is apparently the best Operating mode. This is due to imposing quasi-square-wave on the primary and secondary voltage of the transformer results in trapezoidal, triangular, and sinusoidal waveforms of inductor current in the DAB converter AC link. These modes are advantageous in extending the low-power operating range of the converter [13]. Although these styles tend to thin out the switching losses, the potential loss is important due to zero voltage periods in the quasi-square-wave, which cuts down the effective power transfer at high-power stages.

3. Battery Energy Storage System

BESS is a significant part of PHEV. In this paper, the Pb-acid battery is proposed for energy storage system. Charging and discharging are the two modes of operation of the battery. Modes are desired by the path of current flow into or from the battery. In the modeling of battery, the following parameters were applied [15]. SOC varies linearly with V_{ocb} (open-circuit battery voltage).

SOC (%) is the available charge.

SOCi is the initial state of charge,

SOCm is the uttermost state of complaint.

Ns is the number of cells in series.

As the terminal voltage of the battery is given by

$$V_{bat}=V_{eq}+I_{bat}\,R_{eq} \qquad (1)$$

In (1) V_{bat} and I_{bat} are battery voltage and current, R_{eq} is the equivalent resistance of the battery. V_{eq} and R_{eq} both depend on the mode of battery operation and have different equations. Battery current; I_{bat} is positive when the battery is in charge (ch) mode and negative when it is in the discharge (dch) mode.

In charge mode, R_{eq} and V_{eq} are written as [16],

$$R_{eq} = R_{ch} = \left(0.758 + \frac{0.139}{[1.06 - SOC(t)]N_s}\right)\frac{1}{SOC_m} \quad (2)$$

$$V_{eq} = V_{ch} = [2 + 0.148SOC(t)]N_s \quad (3)$$

In discharging mode R_{eq} and V_{eq} are written as,

$$R_{eq} = R_{dch} = \left(0.19 + \frac{0.1037}{[SOC(t) - 0.14]N_s}\right)\frac{1}{SOC_m} \quad (4)$$

BUPT

$$V_{eq} = V_{dch} = [1.926 + 0.124SOC(t)]N_s \quad (5)$$

4. Effective Battery Charging Controller

Effective utilization of power and efficiency of the battery are decided by the charging time of a battery. In this paper, SCELIC controller is proposed for effectual charging. The efficacy of proposed charging method is analyzed by means of the ANFIS controller.

4.1 ANFIS based Battery Charging Controller

The fuzzy rules are based on human knowledge and consequently for the same performance of the scheme rules will vary from person to person. Still, the major dilemma of FLC is the lack of design practice. The choice of suitable membership functions and choosing the exact rule base needy on the condition is understood with the aid of an ANFIS controller and it is proposed to generate a triggering pulse of DAB bidirectional converter. The ability to learn fuzzy logic is based on an expert's thinking is the solution offered by neural networks. SOC error is fed as input. Basic diagram of ANFIS controller is shown in Figure 3.

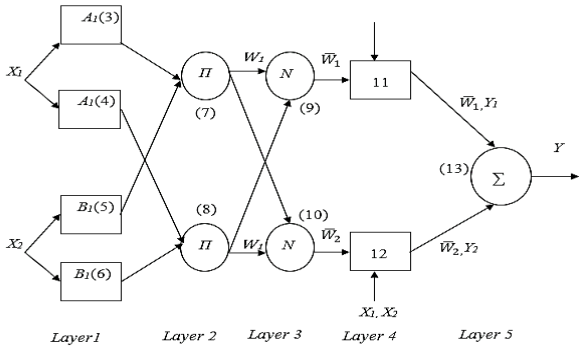


Fig.3 Basic diagram of ANFIS controller.

ANFIS is a Takagi-Sugeno model based fuzzy inference system. This model utilizes specific output and input information set to create fuzzy inference system. At first, for learning of ANFIS, a training data set that consists of the required output/input data pairs of objective systems to be designed is significant. The design factors essential for ANFIS training are training data sets, data pairs, checking data sets and fuzzy inference system. To commence ANFIS training, a number of epochs are selected. The learning results are confirmed subsequent to performing all 25 steps which depend on numerous rules. The considered ANFIS has two inputs such as, the error and change in error of SOC whereas the output is the reference for PWM, it is given to control DAB. In this analysis membership functions of the triangular shape is used.

The fuzzy neural network consists of a five-layer function using feedforward method. ANFIS is a Takagi-Sugeno model based fuzzy inference system and this method designed with two inputs and output data set to make fuzzy inference system. To begin the ANFIS learning primary training information that holds the mandatory output/input data pairs of objective methods to be modeled is necessary. The quantity of data pairs, checking data sets, training data sets, fuzzy inference systems for training, several epochs to be chosen to begin the training, learning results to be established after mentioning the step size is made through the design factors for any ANFIS controller [17].

It is a five-layer feed forward fuzzy neural network. Every layer has its separate importance. Layer 1 (Input Layer): Input layer corresponds to input that is a variable of a controller, which is a SOC error and its variation ratio denoted as x1, x2. This layer gives the input values xi to the subsequent layer, where i = 1 to n Layer 2 (Fuzzification Layer): this layer consists of membership functions that observe the weights of every membership functions (MFs). It obtains the input from the 1st layer and functions as MFs to depict the fuzzy sets of the input variables. Additionally, it performs the membership values which specify the degree to which the input value Xi be in the correct place to the fuzzy set, which operates as the inputs to the subsequent layer.

Layer 3 (Rule layer): every node (every neuron) in this layer performs the prerequisite consequent of the fuzzy rules, i.e., it calculates all rule activation, the number of fuzzy rules and the number of layers being must be equal. Every node of these layers computes the weights which are normalized.

Layer 4 (Defuzzification Layer): It gives the output values "y" obtained from the implication of rules. Connections among the Layer 3 &Layer 4 are weighted by the fuzzy singletons that correspond to an additional set of parameters for the fuzzy neuro network. Layer 5 (Output Layer): It sums up all the inputs coming from the layer 4 and transforms the fuzzy classification results into a crisp value.

4.1.1 Analysis of the Battery charging controller with designed ANFIS controller

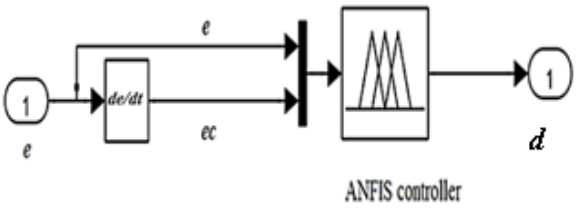


Fig. 4. ANFIS controller Simulink model.

Figure 4 shows ANFIS controller simulink model and Figure 5 shows the training result of ANFIS controller. The battery charging controller is controlled using ANFIS controller. Membership function factors of ANFIS have been tuned with the help neuro-adaptive learning methods. ANFIS controller processes error e and change in error of SOC to decide the pulse width of DAB in PHEV. The choice of the appropriate rule base depending upon the condition is attained by means of an ANFIS controller. The factor of ANFIS

BUPT

controller is resolved by a training procedure that desires three data, such as two input data (SOC error e and change in error ec) and an output data which is the PWM signal to the DAB in PHEV. Once the network is trained, an ANN can be functioned with fresh data and inferences can be produced.

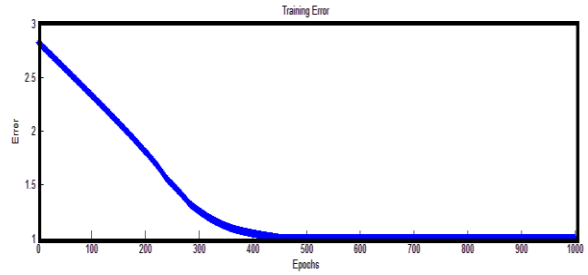


Fig. 5.Training result by ANFIS controller.

By replicating this procedure numerous times the network is trained. The aspire of training is to attain an optimum solution depends on concert measurements. The optimum result attained subsequent to the training shows that the minimization in SOC error and specifies that the act of the ANFIS controller is improved and easy to execute.

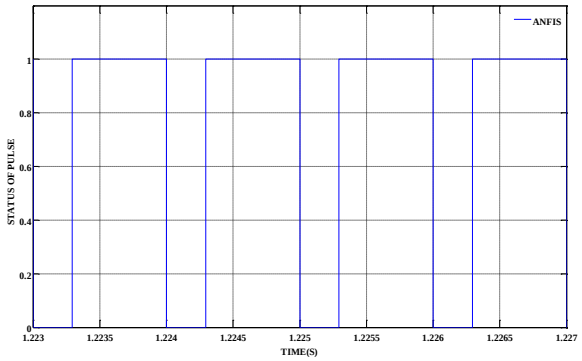


Fig. 6. Triggering pulses from ANFIS controller.

Pulses produced by ANFIS controller for battery charging controller is shown in figure 6.

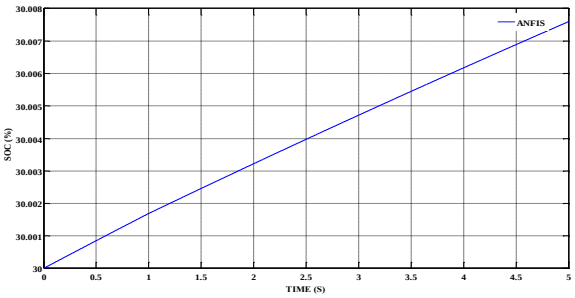


Fig. 7. SOC by the effect of ANFIS based charging controller.

Increasing SOC by the effect of ANFIS based charging controller with initial SOC of 30% is shown in figure 7. Figure 7 is the effect of pulses as in figure 6 produced by the ANFIS based charging controller.

4.2 SCELIC based battery charging Controller

To find out the duty ratio of the battery charging controller, self-computational emotional learning based intelligent controller is proposed in this paper. It mimics the limbic system of a human brain. In the mammalian brain a segment which is mostly accountable for the emotional developments is limbic system [18]. In the cerebral cortex the limbic system is located and consists of subsequent major components, such as sensory cortex, thalamus, amygdala, orbitofrontal cortex, hippocampus and hypothalamus.

The initial step of efficient training of the method emerges in amygdale. It is a tiny almond-structured situated in the sub-cortical zone. It is located in the mode of communicating with each and every other sensory cortical areas contained by the limbic system.

In general, sensory inputs (Si) utter the current situation in which the system is dealing with. In SCELIC sensory input is ANFIS controller which decides the duty ratio initially which is further processed by the following procedure. In a conventional emotional controller sensory input is a non-intelligent controller.

$$A_{th} = \max(S_i) \quad (6)$$

In the model, there is one node A for every sensory input. The maximum stimuli signals are straightly received by means of the path from the thalamus for A_{th} node in the amygdala. This path is stated as a thalamic connection. Thalamic input is not anticipated into the orbitofrontal part and that cannot be inhibited through itself. The output of every node A is estimated depends on the multiplication of pre-defined plastic connection weight V into the analogous input.

$$A_i = S_i V_i \quad (7)$$

In the orbitofrontal cortex, every node O is like A nodes, and the output is intended by relating connection weight (Vi) into the input signal. The connection weight is adjusted proportionally to the deviation amid the commencement of A nodes and the reinforcement signal (emotional signal) R_{ew}. The term R_{ew} is a stable used to regulate the speed of learning. The deviation amongst the reinforcement signal and commencement of the A nodes concludes the revising of the connection weight which at last directs to the learning procedure in the amygdala. The rate of learning is mentioned by the term α

$$\Delta V_i = \alpha\left(S_i \max\left(0, Rew - \sum_j A_j\right)\right) \quad (8)$$

The variation in the connection weights is only incrementing. This is the major motive for the design since one time it learns an emotional response; it has to be everlasting and cannot be unlearned. The O nodes act proportionally, by means of a connection weight W working to the input signal to develop an output.

$$O_i = S_i W_i \quad (9)$$

BUPT

In an orbitofrontal cortex i_{th} value is O_i, in the sensory input i_{th} value is S_i, and in the connection weight i_{th} value is Wi. ΔW_i is measured as,

$$\Delta W_i = \beta\left(S_i(E' - Rew)\right) \quad (10)$$

Orbitofrontal cortex learning rate constant is β. The node *E* simply adds the outputs of the nodes *A* and then subtracts the inhibitory outputs from the nodes *O*. The consequence is the output of the model. The nodes *A* give outputs proportional to their contribution to the prediction of the *Rew* reward, while the nodes *O* inhibit the output of *E* as necessary. The node *E'* is the sum of outputs of *A* except A_{th} and then subtracted from the inhibitory outputs of the nodes *O*. In (8), the term *max* articulates the weight (V_i) that cannot be minimized. The conspicuous evidence for the advantage of this model is that one time the reaction learned by amygdala, it is to be maintained forever. It states that the amygdala cannot disregard the emotional evaluation. Normally, orbitofrontal cortex brings the exception of improper reaction. The orbitofrontal cortex learning rule is computed depends on the assessment among the expected and received reinforcement signal and reduces the model output if there is a variance.

$$E = \sum_{i=0}^{n} A_i - \sum_{i=0}^{n} O_i \text{ (including } A_{th}) \quad (11)$$

$$E' = \sum_{i=0}^{n} A_i - \sum_{i=0}^{n} O_i \text{ (excluding } A_{th}) \quad (12)$$

Revising the adaptive weights in orbitofrontal cortex is nearly analogous to the rule of the amygdala. The distinctive point is that for following the improper response from the amygdala, the orbitofrontal weights must be altered. The *A* nodes make their outputs proportionally to their role in estimating the stress or reward, while the *O* nodes avert the output of *E* if mandatory. The model output D is the variation amongst the output of amygdala and orbitofrontal nodes. Model output D decides the charging time of a battery. To produce triggering pulses, high frequency saw tooth wave is compared with the output of the SCELIC controller. Pulses produced by SCELIC controller for battery charging controller is shown in figure 8.

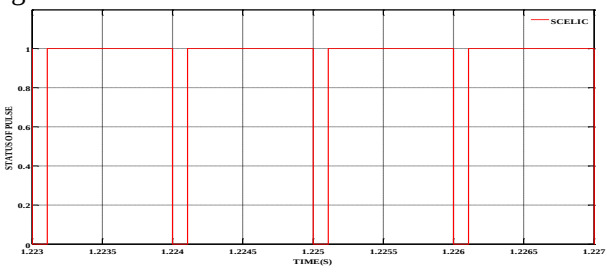


Fig. 8. Triggering pulses from SCELIC.

Increasing SOC by the effect of SCELIC based charging controller with initial SOC of 30% is shown in figure 9.

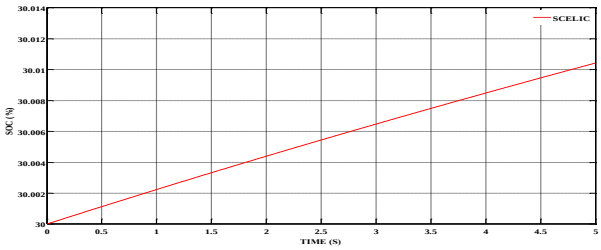


Fig. 9. SOC by the effect of SCELIC based charging controller.

Figure 9 is the effect of pulses as in figure 8 produced by the SCELIC based charging controller.

5. Simulation Results and Discussion

The bidirectional converter runs the motor supplies from the battery. Meantime, it charges the battery when motor acts as a generator. Entire simulation is analyzed using MATLAB/Simulink. The Charging controller decides the efficiency of charging and effectively utilizes the energy generated in the short period from the motor.

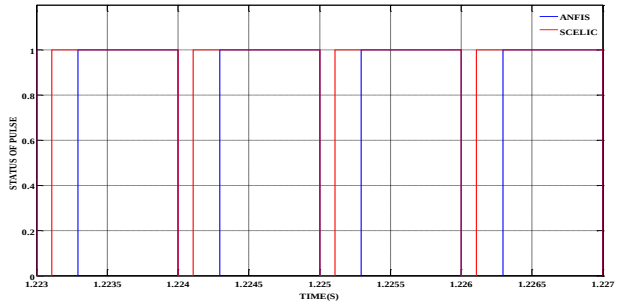


Fig. 10. Assessment of pulses of ANFIS controller and SCELIC.

The assessment of pulses of ANFIS controller and SCELIC is pictured in figure 10. Figure 11 shows the SOC response of batteries with the help of ANFIS and SCELIC based charging controller.

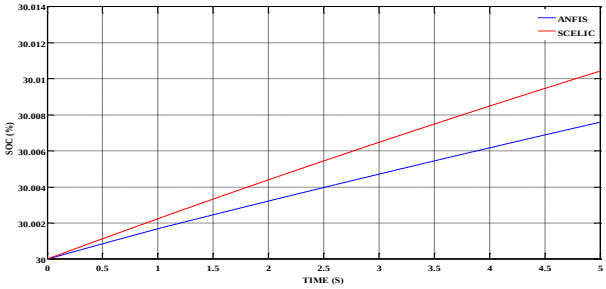


Fig. 11. Assessment of the SOC of batteries using ANFIS and SCELIC.

From the figure 10, it is clear that the charging controller pulse width produced by SCELIC is improved compared to the ANFIS controller. It results that SCELIC based charging controller charges the battery quickly than ANFIS controller as shown in Figure 11.

BUPT

6. Conclusion

In this paper novel SCELIC controller is proposed as charging controller in the battery of PHEV. Energy consumed by PHEV is decided by the charging of battery which decides the efficiency and performance of PHEV. A high power, the bidirectional DC-DC converter is introduced in PHEV to charge the battery when the motor in PHEV acts as a generator. This method of charging reduces power consumption from the grid and reduces problems associated with sudden load demand (PHEV charging) in a grid. In this paper novel SCELIC controller is proposed to reduce charging time which improves the performance of charging and reduces energy consumed from the grid. Artificial intelligent ANFIS controller is analyzed as charging controller and it is compared with proposed SCELIC. From Matlab simulation comparative analysis it is validated that proposed SCELIC controller improves charging performance compare to ANFIS which efficiently consumes the power from the motor for its battery in PHEV and decreases load demand on the Distribution grid.

References

1. Yonghua Song, Xia Yang, Zongxiang Lu, 2010. Integration of Plug-in Hybrid and Electric Vehicles: Experience from China. *IEEE Power and Energy Society General Meeting*, pp.1-6.
2. Faria, R., Moura, P., Delgado, J. and De Almeida, A.T., 2012. A sustainability assessment of electric vehicles as a personal mobility system. *Energy Conversion and Management*, *61*, pp.19-30.
3. Karden, E., Ploumen, S., Fricke, B., Miller, T. and Snyder, K., 2007. Energy storage devices for future hybrid electric vehicles. *Journal of Power Sources*, *168*(1), pp.2-11.
4. Zhang, B., Mi, C.C. and Zhang, M., 2011. Charge-depleting control strategies and fuel optimization of blended-mode plug-in hybrid electric vehicles. *IEEE Transactions on Vehicular Technology*, *60*(4), pp.1516-1525.
5. Papadaskalopoulos, D., Strbac, G., Mancarella, P., Aunedi, M. and Stanojevic, V., 2013. Decentralized participation of flexible demand in electricity markets—Part II: Application with electric vehicles and heat pump systems. *IEEE Transactions on Power Systems*, *28*(4), pp.3667-3674.
6. Krismer, F., 2010. *Modeling and optimization of bidirectional dual active bridge DC-DC converter topologies* (Doctoral dissertation, ETH Zurich).
7. Nan, C. and Ayyanar, R., 2013, September. Dual active bridge converter with PWM control for solid state transformer application. In *Energy Conversion Congress and Exposition (ECCE), 2013 IEEE* (pp. 4747-4753). IEEE.
8. Rodriguez, A., Vazquez, A., Lamar, D.G., Hernando, M.M. and Sebastian, J., 2015. Different purpose design strategies and techniques to improve the performance of a dual active bridge with phase-shift control. *IEEE Transactions on Power Electronics*, *30*(2), pp.790-804.
9. Ortiz, G., Uemura, H., Bortis, D., Kolar, J.W. and Apeldoorn, O., 2013. Modeling of soft-switching losses of IGBTs in high-power high-efficiency dual-active-bridge DC/DC converters. *IEEE Transactions on Electron Devices*, *60*(2), pp.587-597.
10. Lucas, C., Shahmirzadi, D. and Sheikholeslami, N., 2004. Introducing BELBIC: brain emotional learning based intelligent controller. *Intelligent Automation & Soft Computing*, *10*(1), pp.11-21.
11. Ang, S.S. and Converters, P.S., 1995. New York: M.
12. Jain, A.K. and Ayyanar, R., 2011. PWM control of dual active bridge: Comprehensive analysis and experimental verification. *IEEE Transactions on Power Electronics*, *26*(4), pp.1215-1227.
13. Haihua, Z. and Khambadkone, A.M., 2008, October. Hybrid modulation for dual active bridge bi-directional converter with extended power range for ultracapacitor application. In *Industry Applications Society Annual Meeting, 2008. IAS'08. IEEE* (pp. 1-8). IEEE.
14. Oggier, G., Garcia, G.O. and Oliva, A.R., 2011. Modulation strategy to operate the dual active bridge DC–DC converter under soft switching in the whole operating range. *IEEE Transactions on Power Electronics*, *26*(4), pp.1228-1236.
15. Kalantar, M., 2010. Dynamic behavior of a stand-alone hybrid power generation system of wind turbine, microturbine, solar array and battery storage. *Applied energy*, *87*(10), pp.3051-3064.
16. Chin C.S., Babu, A. and McBride, W., 2011. Design, modeling and testing of a standalone single axis active solar tracker using MATLAB/Simulink. *Renewable Energy*, *36*(11), pp.3075-3090.
17. Awadallah, M.A., Bayoumi, E.H. and Soliman, H.M., 2009. Adaptive deadbeat controllers for brushless DC drives using PSO and ANFIS techniques. *Journal of Electrical Engineering*, *60*(1), pp.3-11.
18. Mohammdi-Milasi, R.A.S.O.U.L., Lucas, C. and Najar-Arrabi, B., 2004, June. A novel controller for a power system based BELBIC (brain emotional learning based intelligent controller). In *Automation Congress, 2004. Proceedings. World* (Vol. 16, pp. 409-420). IEEE.

BUPT